Structural and Photophysical Properties of [(CO)3(phen)Re(μ-Br)Re(phen)(CO)3]+ [(CO)3Re(μ-Br)3Re(CO)3]−: where does its luminescence come from?

ARTICLE *in* POLYHEDRON · MAY 2015

Impact Factor: 2.01 · DOI: 10.1016/j.poly.2015.05.024

7 AUTHORS, INCLUDING:

Santi Nonell

Universitat Ramon Llull

171 PUBLICATIONS **2,570** CITATIONS

SEE PROFILE

German Gunther

University of Chile

45 PUBLICATIONS **314** CITATIONS

SEE PROFILE

Eduardo Chamorro

Universidad Andrés Bello

79 PUBLICATIONS **1,604** CITATIONS

SEE PROFILE

Nancy Pizarro

Universidad Andrés Bello

24 PUBLICATIONS **117** CITATIONS

SEE PROFILE

Polyhedron 97 (2015) 227–233

Contents lists available at ScienceDirect

Polyhedron

journal homepage: www.elsevier.com/locate/poly

Structural and photophysical properties of $[(CO)_3(phen)Re(\mu\text{-}Br)Re(phen)(CO)_3]^+[(CO)_3Re(\mu\text{-}Br)_3Re(CO)_3]^-$: Where does its luminescence come from?

Hector Gallardo [a], Marjorie Cepeda-Plaza [a], Santi Nonell [b], Germán Günther [c], Eduardo Chamorro [a], Nancy Pizarro [a], Andrés Vega [d,e,*]

[a] Universidad Andres Bello, Facultad de Ciencias Exactas, Departamento de Ciencias Químicas, Av. República 275, 3er Piso, Chile
[b] Universitat Ramon Llull, Institut Quimic de Sarrià, Via Augusta, 390, E-08017 Barcelona, Spain
[c] Universidad de Chile, Facultad de Ciencias Químicas y Farmacéuticas, Sergio Livingstone 1007, Santiago, Chile
[d] Universidad Andres Bello, Facultad de Ciencias Exactas, Departamento de Ciencias Químicas, Quillota 980, Viña del Mar, Chile
[e] Centro para el Desarrollo de la Nanociencia y la Nanotecnología, CEDENNA, Chile

ARTICLE INFO

Article history:
Received 2 April 2015
Accepted 15 May 2015
Available online 27 May 2015

Keywords:
Re^I
Multimetallic complex
Cation
Crystal structure
Luminescence

ABSTRACT

The multimetallic complex $[[(CO)_3(phen)Re(\mu\text{-}Br)Re(phen)(CO)_3][(CO)_3Re(\mu\text{-}Br)_3Re(CO)_3]]\cdot CH_2Cl_2$ was prepared by direct reaction of $(Re(CO)_3(THF)Br)_2$ (THF: tetrahydrofuran) and 1,10-phenanthroline in a 1:1 ratio, followed by recrystallization in dichloromethane. The compound is an ionic salt where both, cation and anion, are bimetallic complexes. Inside both of them the Re^I centers are bridged by one or three bromides respectively. The compound has an absorption band centered at 375 nm in CH_2Cl_2, which has been assigned to a MLCT band. Excitation at 375 nm produces luminescent emission at 608 nm. Comparison of these results with closely related rhenium complexes, in addition to Time Dependant-DFT analysis, allow us to propose the $[(CO)_3(phen)Re(\mu\text{-}Br)Re(phen)(CO)_3]^+$ cation as main responsible for luminescence. Luminescence lifetime and singlet oxygen formation quantum yield suggest also that the emissive excited state has a triplet character.

1. Introduction

Rhenium(I) tricarbonyl diimine complexes, $[(N,N)Re(CO)_3(X)]$ (X = halide), have received considerable attention in the last years due to their interesting photophysical and photochemical properties, which can be tuned by modifying either the nature of diimine ligand (N,N) or the L ligand itself (Cl, Br) [1–5]. These structural changes have direct influence on the character of the excited states [6,7]. One of the most simple chelating diimine ligands is 1,10-phenanthroline (*phen*), which was the ligand in the first Re^I tricarbonyl diimine complex described in early 1941 [8]. From a synthetic point of view, the rhenium diimine complexes are usually accessible in good yields and reasonable purity by the direct reaction of the diimine ligand with the rhenium carbonyl halide $Re(CO)_5X$ (X = Cl, Br) in an inert solvent. However, this widely used synthetic path implies refluxing, which can cause some problems such as low yields or generation of by-products. Also, an affordable synthetic strategy is the use of $\{N(C_4H_9)_4\}_2[Re(CO)_3Br_3]$ instead of $Re(CO)_5X$ [9]. Alternatively, we have recently described the reaction of the dimeric precursor $[(CO)_3(THF)Re(\mu\text{-}Br)_2Re(THF)(CO)_3]$ with 2-pyridylphosphine at room temperature to give the mononuclear complex *P,N*-$\{(C_6H_5)_2(C_5H_4N)P\}Re(CO)_3Br$ in a 61% yield [10]. This simple procedure offers a very attractive synthetic approach that can be widely useful for chelating bidentate ligands, and can also be used as a general route to obtain Re^I complexes at room temperature. Based on this previous knowledge, we carried out the synthesis using 1,10-phenanthroline (*phen*) as chelating ligand instead the aforementioned phosphine. We predicted the reaction would certainly render the $[(phen)Re(CO)_3Br]$ complex, but surprisingly, we found that reaction led us to the multimetallic salt $[(CO)_3(phen)Re(\mu\text{-}Br)Re(phen)(CO)_3]^+[(CO)_3Re(\mu\text{-}Br)_3Re(CO)_3]^-$ as the main reaction product. In this work, we report the structural and photophysical properties of this new complex in terms of its molecular structure, supplemented by DFT and time-dependent DFT calculations. Considering the presence of two different types of Re^I centers, we discuss in detail about the molecular fragment responsible for the luminescent properties of this multimetallic complex and how these properties can be related to its structurally analogous monomeric complex $[(phen)Re(CO)_3Br]$.

* Corresponding author at: Universidad Andres Bello, Facultad de Ciencias Exactas, Departamento de Ciencias Químicas, Quillota 980, Viña del Mar, Chile. Tel.: +56 322845192.
E-mail address: andresvega@unab.cl (A. Vega).

http://dx.doi.org/10.1016/j.poly.2015.05.024
0277-5387/

2. Experimental

All reagents, $(Re(CO)_3(THF)Br)_2$ (THF: tetrahydrofuran) and 1,10-phenanthroline were used as received from the supplier (Aldrich), with no purification before use. Solvents were dried and freshly distilled before use. Standard Schlenk techniques were used for all manipulations.

2.1. Synthesis of $[[(CO)_3(phen)Re(\mu\text{-}Br)Re(phen)(CO)_3][(CO)_3Re(\mu\text{-}Br)_3Re(CO)_3]]\cdot CH_2Cl_2$

The compound was prepared by the direct reaction of $(Re(CO)_3(THF)Br)_2$ and 1,10-phenanthroline in the stoichiometric relation 1:1 at room temperature, according to Scheme 1:

A colorless solution of 91 mg of the ligand 1,10-phenanthroline (0.505 mmol) in toluene was added dropwise to a colorless solution of 475 mg (0.505 mmol) of $(Re(CO)_3Br(THF))_2$ dissolved in 20 mL of toluene. After the addition was completed, another 20 mL of toluene were added to the reaction mixture. Reaction was stirred at room temperature overnight. Toluene was eliminated from the reaction mixture by evaporation at reduced pressure. A yellow crude material was obtained after evaporation. Re-crystallization of the material was carried out in a CH_2Cl_2/hexane mixture (1:1). 200 mg of homogenous crystalline material from which an X-ray quality single crystal was selected for the diffraction experiment (45%). The use of a normal stoichiometry 1:2 precursor/diimine leads to the normal monomeric complex [(*phen*)Re(CO)$_3$Br] [11].

Anal. Calc. for $C_{37}H_{18}Br_4Cl_2N_4O_{12}Re_4$: C, 24.08%; H, 0.98%; N, 3.04%. Found: C, 24.50%; H, 0.96%; N, 2.90%. Elemental analyses were obtained at Centro de Ensayos y Estudios Externos de Química, CEQUC at Pontificia Universidad Católica de Chile.

IR (cm^{-1}): 2060 (s), 1970(s), 1950(s), 1460.

2.2. Photophysical measurements

UV–Vis spectra were recorded on an Agilent 8453 Diode-Array spectrophotometer in the range of 250–600 nm in aerated dichloromethane solutions. Emission spectra were measured in a Horiba Jobin-Yvon FluoroMax-4 spectrofluorometer at room temperature. Luminescence lifetime measurements were carried out with the time correlated single photon counting technique using either an Edinburgh Instruments OB-900 or a PicoQuant FluoTime 200 fluorescence lifetime spectrometer. A LDH-P-C-375 laser was employed as the pulsed light source (FWHM ~ 70 ps; average power 0.5 mW). Generation of singlet oxygen, ($O_2(^1\Delta_g)$), was monitored at 1270 nm using a Hamamatsu NIR-PMT detector (H9170-45), using a diode-pumped pulsed Nd:YAG laser (FTSS355-Q; Crystal Laser, Berlin, Germany) working at 10 kHz repetition rate for excitation. Quantum yields of $O_2(^1\Delta_g)$ generation were measured at room temperature using perinaphthenone as actinometer (ϕ_Δ = 0.95 in DCM) [12]. Experiments were carried out in either air-equilibrated or argon-saturated dichloromethane solutions. It is important to emphasize the very limited solubility of the complex, which precludes additional experiences like cyclic voltammetry.

2.3. X-rays diffraction

The crystal structure of $[(CO)_3(phen)Re(\mu\text{-}Br)Re(phen)(CO)_3]^+$ $[(CO)_3Re(\mu\text{-}Br)_3Re(CO)_3]^-$ was determined by X-rays diffraction on a plate-shaped 0.19 × 0.12 × 0.12 mm^3 single crystal at 273 K. Data collection was done on a SMART CCD diffractometer using ω-scans as collection strategy. Data was reduced using SAINT [13], while the structure was solved by direct methods, completed by Difference Fourier Synthesis and refined by least-squares using SHELXL [14]. Multi-scan absorption corrections were applied using SADABS [13]. The hydrogen atoms positions were calculated after each cycle of refinement with SHELXL using a riding model for each structure, with C–H distance of 0.95 Å. $U_{iso}(H)$ values were set equal to 1.2 U_{eq} of the parent carbon atom. Table 1 contains details of crystal and refinement parameters.

2.4. Computational details

All geometry optimizations were performed at the B3LYP/6-31 + G(d,p) level of theory using the Gaussian09 Rev C.01 package of programs (G09) [15], and started from geometry determined by means of X-Ray diffraction. The LANL2DZ basis set was used only for rhenium. Excited state calculations were performed within the Time-Dependent DFT (TD-DFT) methodology as implemented in G09. Solvent effect for simulating dichloromethane has been incorporated through the polarizable continuum model (PCM)

Table 1
Crystal data and structure refinement for $[(CO)_3(phen)Re(\mu\text{-}Br)Re(phen)(CO)_3]^+$ $[(CO)_3Re(\mu\text{-}Br)_3Re(CO)_3]^-$.

FW/uma	1845.89
Crystal System	Monoclinic
Space Group	$P2_1/n$
a (Å)	16.325(4)
b (Å)	16.628(5)
c (Å)	17.880(5)
β (°)	108.296(4)
V (Å^3)	4608 (2)
Z	4
d (g cm^{-3})	2.661
μ (mm^{-1})	14.12
$F(000)$	3352.0
θ range	2.4–26.5°
hkl range	$-20 \leqslant h \leqslant 20$ $-20 \leqslant k \leqslant 20$ $-21 \leqslant l \leqslant 22$
N_{tot}, N_{uniq}	31,939, 9539
(R_{int}), N_{obs}	(0.0595), 6672
Refinement parameters	568
Goodness-of-fit (GOF)	0.92
R_1, wR_2 (obs)	0.0420, 0.0769
R_1, wR_2 (all)	0.0667, 0.0829
Maximum and minimum $\Delta\rho$	2.54 and −2.94

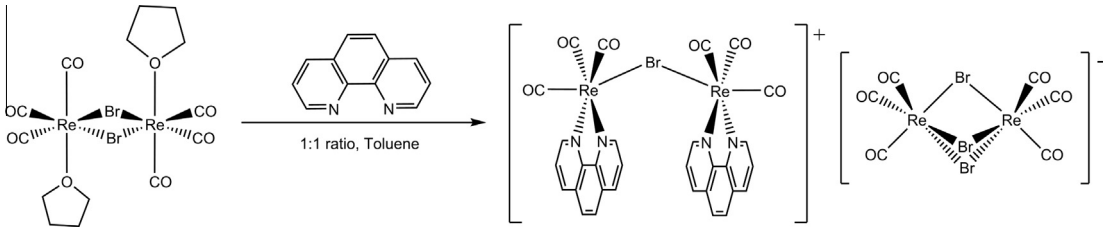

Scheme 1. Schematic synthetic path of $[[(CO)_3(phen)Re(\mu\text{-}Br)Re(phen)(CO)_3][(CO)_3Re(\mu\text{-}Br)_3Re(CO)_3]]\cdot CH_2Cl_2$.

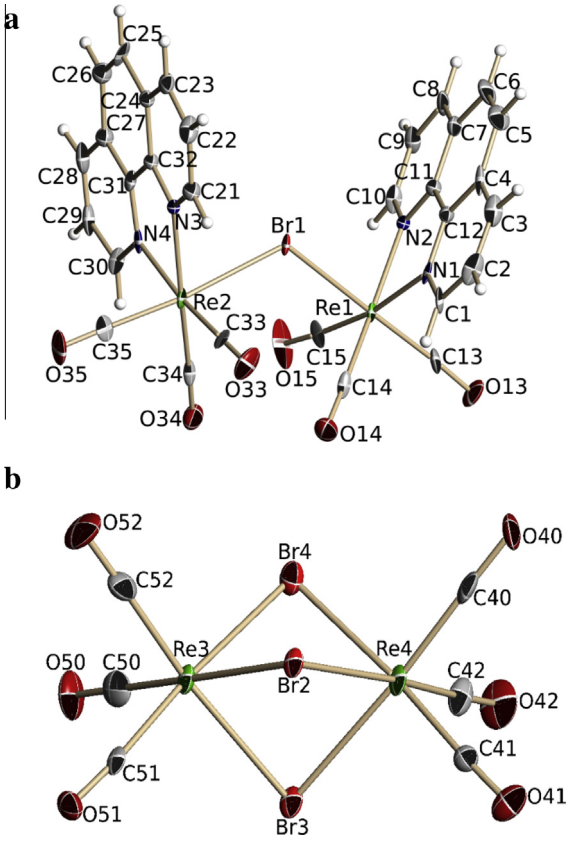

Fig. 1. Molecular structure diagram for: (a) the $[(CO)_3(phen)Re(\mu\text{-}Br)Re(phen)(CO)_3]^+$ cation and (b) the $[(CO)_3Re(\mu\text{-}Br)_3Re(CO)_3]^-$ anion, both showing partial atom numbering scheme. Displacement ellipsoids drawn at the 50% level of probability.

Table 2
Bond distances (Å) and angles (°) for $[(CO)_3(phen)Re(\mu\text{-}Br)Re(phen)(CO)_3]^+[(CO)_3Re(\mu\text{-}Br)_3Re(CO)_3]^-$.

Re1–C14	1.900 (9)	Re1–Br1	2.6450 (10)
Re1–C13	1.908 (9)	Re1–N1	2.181 (7)
Re1–C15	1.881 (9)	Re1–N2	2.183 (6)
Re2–N3	2.163 (6)	Br1–Re2	2.6604 (10)
Re2–N4	2.195 (7)	Re1–Re2	4.5866 (10)
Re3–Br2	2.6662 (11)	Re3–Re4	3.5069 (10)
Re3–Br3	2.6621 (11)	Br2–Re4	2.6673 (11)
Br4–Re4	2.6386 (11)	Br3–Re4	2.6612 (11)
Re3–Br4	2.6398 (11)		
C14–Re1–N1	97.8 (3)	C13–Re1–N1	96.4 (3)
C15–Re1–N1	171.3 (3)	C14–Re1–N2	172.7 (3)
C13–Re1–N2	95.6 (3)	C15–Re1–N2	97.7 (3)
N1–Re1–N2	75.8 (2)	C14–Re1–Br1	90.7 (3)
C13–Re1–Br1	177.2 (3)	C15–Re1–Br1	92.7 (3)
N1–Re1–Br1	80.99 (18)	N2–Re1–Br1	84.71 (17)
C33–Re2–N3	97.7 (3)	C34–Re2–N3	171.7 (3)
C35–Re2–N3	94.7 (3)	C33–Re2–N4	172.8 (3)
C34–Re2–N4	97.3 (3)	C35–Re2–N4	94.7 (3)
N3–Re2–N4	75.5 (3)	C33–Re2–Br1	91.5 (3)
C34–Re2–Br1	97.2 (3)	C35–Re2–Br1	172.8 (3)
N3–Re2–Br1	78.25 (18)	N4–Re2–Br1	84.91 (17)
Br4–Re3–Br2	81.15 (3)	Br4–Re4–Br2	81.15 (3)
Br3–Re3–Br2	79.97 (3)	Br3–Re4–Br2	79.96 (3)

using the integral equation formalism variant (IEFPCM) [16,17]. Absorption and emission spectra were simulated from the above calculations using the GaussSum 3.0 suite of freely available processing tools. A full width at half-maximum (FWHM) of the Gaussian curves corresponding to 3000 cm^{-1} was employed to convolute both spectra. Representations for molecular orbitals were generated using the G09 cubegen tool and visualization was obtained using VMD and Povray 3.6 programs [18,19]. Electron-donor and electron-acceptor intrinsic electronic responses were evaluated by calculating Fukui functions $f^-(r)$ and $f^+(r)$, respectively [20], obtained within a condensed-to-atom framework [21]. The simple formalism based on the linear expansion of the frontier molecular orbitals in a given basis-set has been employed as reported elsewhere [22–24].

3. Results and discussion

3.1. Structural description

The structure of the compound corresponds to an ionic salt, bearing a bimetallic cation, $[(CO)_3(phen)Re(\mu\text{-}Br)Re(phen)(CO)_3]^+$; and a bimetallic $[(CO)_3Re(\mu\text{-}Br)_3Re(CO)_3]^-$ anion. Thus, cation and anion present two different types of Re^I centers within the crystal structure of the complex; one is the $(CO)_3(phen)ReBr$ found

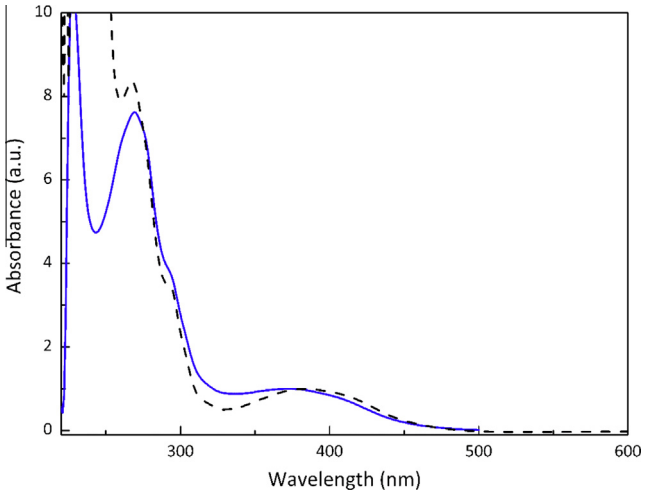

Fig. 2. Absorption spectra for $[(CO)_3(phen)Re(\mu\text{-}Br)Re(phen)(CO)_3]^+[(CO)_3Re(\mu\text{-}Br)_3Re(CO)_3]^-$ (solid blue line) and for the monomer $[(phen)Re(CO)_3Br]$ (dashed black line), both measured in air-equilibrated CH_2Cl_2 solution. (Colour online.)

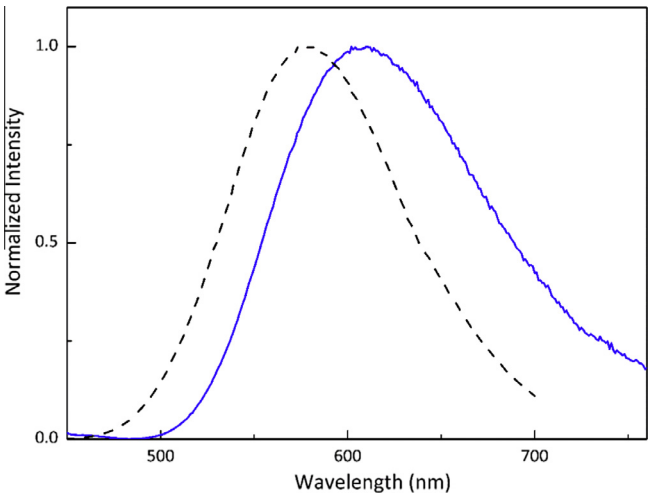

Fig. 3. Normalized emission spectra of $[(CO)_3(phen)Re(\mu\text{-}Br)Re(phen)(CO)_3]^+[(CO)_3Re(\mu\text{-}Br)_3Re(CO)_3]^-$ (solid blue line) and the monomer $[(phen)Re(CO)_3Br]$ (dashed black line) measured in air-equilibrated CH_2Cl_2 at room temperature (λ_{exc} = 375 nm). (Colour online.)

at the cationic portion and the other, $(CO)_3ReBr_3$ found at the anion. At the $[(CO)_3(phen)Re(\mu\text{-}Br)Re(phen)(CO)_3]^+$ cation, two organometallic $[Re(phen)(CO)_3]^+$ fragments are bonded through a single bromide bridge; while at $[(CO)_3Re(\mu\text{-}Br)_3Re(CO)_3]^-$ anion, the two organometallic $[Re(CO)_3]^+$ fragments are bonded through three bromide anions (Table 2). Consequently, the coordination environment for each Re^I center within both ions can be described as non-regular octahedrons. In the cation $[(CO)_3(phen)Re(\mu\text{-}Br)Re(phen)(CO)_3]^+$ (Fig. 1a), two octahedral Re^I centers are defined by a phenanthroline molecule, three carbonyl groups at *fac* positions and the bromide, which is shared by both rhenium sites. In view of these characteristics, the cation can be described as being formed by two vertex sharing octahedrons, with the common vertex being occupied by the bromide. The planes defined by each $[Re(phen)]^+$ fragment within the cation are not coplanar, displaying a dihedral angle of 32.7(1)°, as computed from the respective least-squares plane. Additionally, crystal structure shows a distance between the two rhenium centers of 4.5866(10) Å and a Re1-Br1-Re2 angle with a value of 119.65(4)°, revealing an angular conformation around the bromide. To the best of our knowledge, there is no previous evidence of this kind of cation, containing two $[(CO)_3Re(phen)]^+$ moieties bonded through a single halide. Only few similar examples have been found in the literature for the complexes $[(CO)_4\{(C_6H_5)_3P\}Re(\mu\text{-}Cl)Re\{P(C_6H_5)_3\}(CO)_4]^+$ [25] and $[(CO)_2Cp^*Re(\mu\text{-}Br)ReCp^*(CO)_2]^+$ [26]. In the case of the $[(CO)_3Re(\mu\text{-}Br)_3Re(CO)_3]^-$ anion (Fig. 1b), the two octahedral rhenium centers share a face, leading to a considerably shorter distance between the two rhenium centers of 3.507(1) Å.

Although other examples of complexes exhibiting face-sharing octahedral Re^I centers connected by halide, such as chloride and/or bromide anions have been previously described, they correspond mainly to reaction by-products. For instance, the reduction of the rhenium(III) tetracarboxylate $Re_2(O_2CCH_3)_2X_4L_2$ (X = Cl or Br; L = pyridine, H_2O) with *triphos* ($CH_3C(CH_2PPh_2)_3$) led to the bioctahedral dirhenium(II) cation $[Re_2(\mu\text{-}X)_3(triphos)_2]$, where X can be either chloride or bromide [27]. On the other hand, cases where

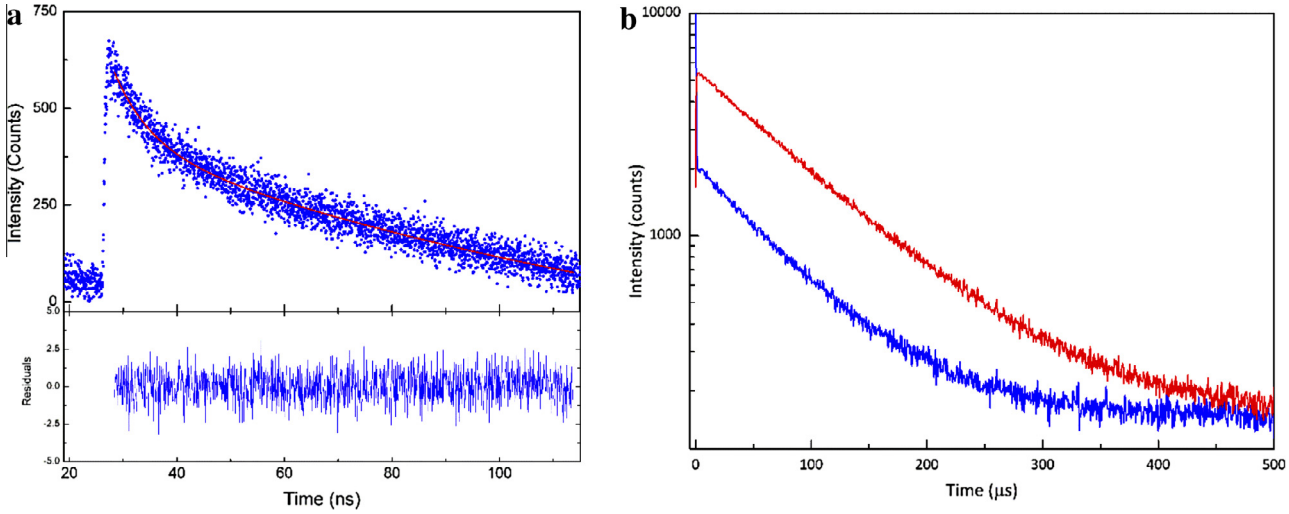

Fig. 4. (a) Time resolved emission decay of $[(CO)_3(phen)Re(\mu\text{-}Br)Re(phen)(CO)_3]^+[(CO)_3Re(\mu\text{-}Br)_3Re(CO)_3]^-$ followed at 600 nm, upon excitation at 375 nm. (b) Direct $O_2(^1\Delta_g)$ detection at 1275 nm, sensitized by $[(CO)_3(phen)Re(\mu\text{-}Br)Re(phen)(CO)_3]^+[(CO)_3Re(\mu\text{-}Br)_3Re(CO)_3]^-$ (blue line) and perinaphthenone (red line) as reference compound, upon excitation at 355 nm. (Colour online.)

Table 3
Summary of main energy, wavelength and oscillator strength, computed for observed transitions in the absorption spectra of the $[(CO)_3(phen)Re(\mu\text{-}Br)Re(phen)(CO)_3]^+$ cation and the $[(CO)_3Re(\mu\text{-}Br)_3Re(CO)_3]^-$ anion, together with the orbitals implied.

Gas phase					PCM: CH_2Cl_2				
N	*E*/eV	*λ*/nm	*f*	Major contributions	*N*	*E*/eV	*λ*/nm	*f*	Major contributions
$[(CO)_3(phen)Re(\mu\text{-}Br)Re(phen)(CO)_3]^+$									
1	2.64	469	0.0057	HOMO → LUMO	1	2.99	415	0.0101	HOMO → LUMO
3	2.95	421	0.0322	HOMO−1 → LUMO + 1 HOMO → LUMO + 2	3	3.25	381	0.0934	HOMO−1 → LUMO + 1 HOMO → LUMO + 2
4	2.95	420	0.0188	HOMO−1 → LUMO + 1 HOMO → LUMO + 3	4	3.27	379	0.0576	HOMO−1 → LUMO + 1 HOMO → LUMO + 3
7	3.05	407	0.0489	HOMO−1 → LUMO + 1 HOMO → LUMO + 1 HOMO → LUMO + 2	7	3.43	362	0.0248	HOMO−1 → LUMO + 1 HOMO → LUMO + 1 HOMO → LUMO + 2
8	3.06	406	0.0453	HOMO−1 → LUMO + 1 HOMO → LUMO + 3	8	3.43	361	0.0346	HOMO−1 → LUMO + 1 HOMO → LUMO + 3
$[(CO)_3Re(\mu\text{-}Br)_3Re(CO)_3]^-$									
1	4.05	306	0.0064	HOMO → LUMO + 1 HOMO → LUMO + 2	6	4.06	305	0.0087	HOMO−1 → LUMO + 3 HOMO → LUMO + 1
8	4.16	298	0.0144	HOMO → LUMO + 3 HOMO → LUMO + 4	8	4.16	298	0.0209	HOMO → LUMO + 3
11	4.34	286	0.0297	HOMO−1 → LUMO + 3 HOMO → LUMO + 2	11	4.33	287	0.0498	HOMO−1 → LUMO + 2 HOMO → LUMO + 1
16	4.80	258	0.0931	HOMO → LUMO + 3 HOMO → LUMO + 4	16	4.80	258	0.1409	HOMO → LUMO+3

the $[(CO)_3Re(\mu\text{-}Br)_3Re(CO)_3]^-$ anion is the counterbalancing charge of some cationic Re^I species are limited to *fac*-$[Re(H_2O)_3(CO)_3]^+$ $[(CO)_3Re(\mu\text{-}Br)_3Re(CO)_3]^-$ [28], and $[(\eta^6\text{-}C_6H_5CH_3)Re(CO)_3]^+[(CO)_3Re(\mu\text{-}Br)_3Re(CO)_3]^-$ [29].

3.2. Spectroscopic properties

The absorption spectrum of the $[(CO)_3(phen)Re(\mu\text{-}Br)Re(phen)(CO)_3]^+[(CO)_3Re(\mu\text{-}Br)_3Re(CO)_3]^-$ complex in aerated dichloromethane solution is shown in Fig. 2. The broad absorption band centered at 375 nm ($\sim 5 \times 10^{-3}\ M^{-1}\ cm^{-1}$), has been assigned to a metal (d_π) to ligand (π^*) charge transfer transition (MLCT). A ligand-centered $\pi\pi^*$ transition (LC) has been discarded since this type of transitions generally occur at shorter wavelengths (below 300 nm) [2,5]. As commented above, almost no examples of this type of multimetallic complex have been found in the literature. Then, to the best of our knowledge, no description of the spectroscopic properties for such species has been published yet. Maybe, the most related point of comparison is the monomeric Re^I complex $[(phen)Re(CO)_3Br]$ [5,11], whose absorption spectrum is also shown in Fig. 2. The multimetallic complex presents a very similar spectrum relative to the monomeric $[(phen)Re(CO)_3Br]$, showing a small blue shift of the MLCT transition band and a more pronounced shoulder centered at 300 nm. The shift can be explained in terms of a diminished donor ability of the bromide atom, which is shared between the two rhenium atoms in the multimetallic

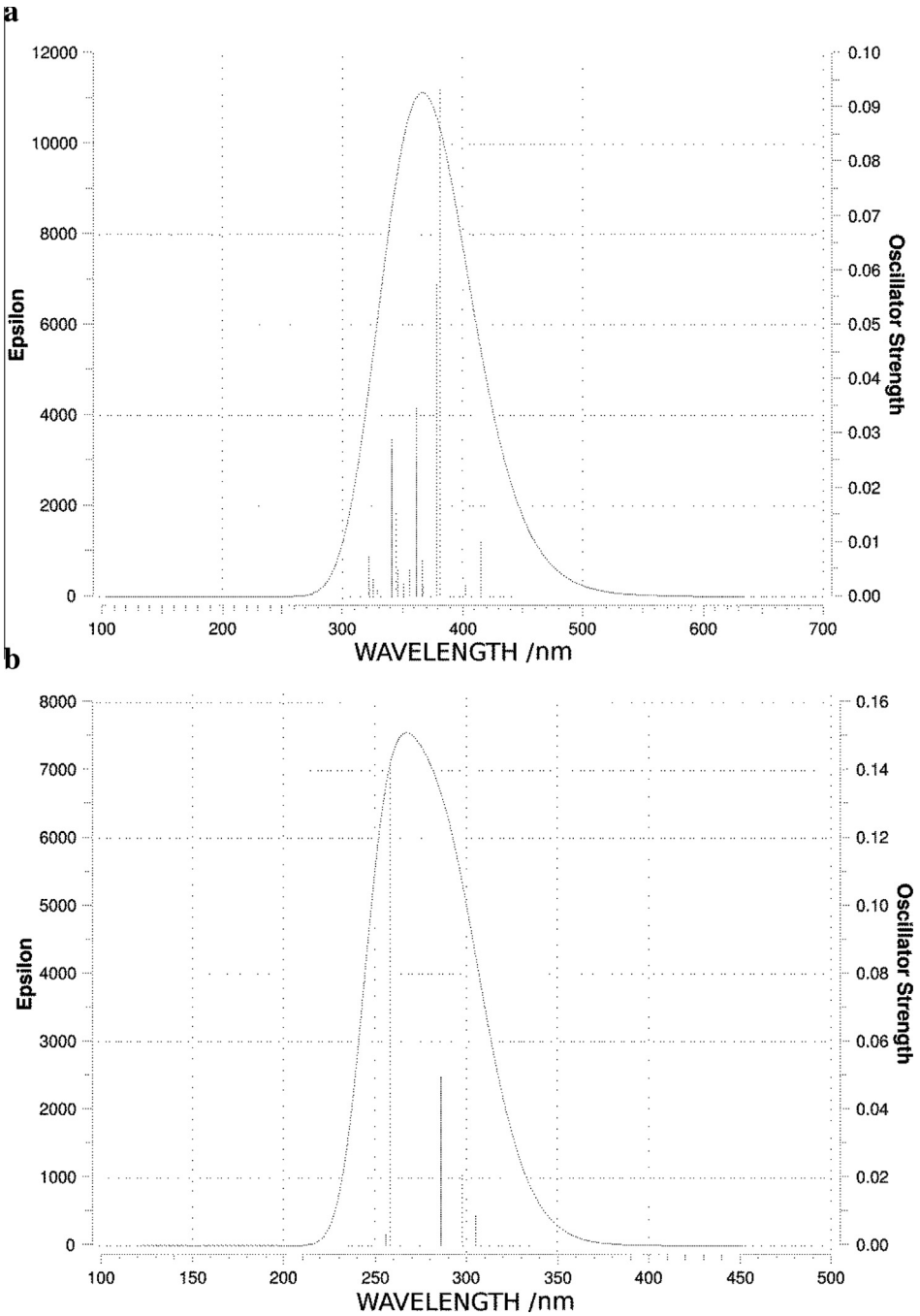

Fig. 5. TD-DFT computed transitions for (a) the $[(CO)_3(phen)Re(\mu\text{-}Br)Re(phen)(CO)_3]^+$ cation and (b) the $[(CO)_3Re(\mu\text{-}Br)_3Re(CO)_3]^-$ anion, using PCM corresponding to CH_2Cl_2.

compound. It has been proposed that higher donor ability of ligands favor the charge transfer transition $d_\pi \rightarrow \pi^*$ (Re oxidation) [1,5].

Fig. 3 shows the emission spectra of both multimetallic $[(CO)_3(phen)Re(\mu\text{-}Br)Re(phen)(CO)_3]^+[(CO)_3Re(\mu\text{-}Br)_3Re(CO)_3]^-$ and monomeric $[(phen)Re(CO)_3Br]$ complexes, upon excitation at 375 nm. The emission spectrum of the multimetallic complex presents a broad band with a maximum centered at 608 nm which is dominated by the MLCT transition. On the other hand, the monometallic compound $[(phen)Re(CO)_3Br]$, shows a blue-shifted emission band centered at 580 nm which is in accordance with emission reported for this kind of complexes [2,4]. Both emission spectra were independent of excitation wavelength. Consecutively, we carried out time-resolved emission measurements on air-equilibrate dichloromethane solutions upon excitation at 375 nm. The results revealed a multi-exponential decay with a short component of 7 ns (20% in amplitude) and a long component of 136 ns (80% in amplitude). Additionally, we were able to identify the capability of generation of $O_2(^1\Delta_g)$ by monitoring the luminescence at 1270 nm, upon irradiation of air-equilibrated solutions at 355 nm. A quantum yield value of 0.330 was calculated using perinaphthenone as actinometer. Fig. 4a and b show the emission decay followed at 600 nm for the multimetallic complex and the direct detection of $O_2(^1\Delta_g)$, sensitized by this compound detected at 1270 nm, both upon excitation at 375 and 355 nm, respectively. These findings are in agreement with the fast intersystem crossing reported for rhenium tricarbonyl diimine complexes, assigning a triplet character to the MLCT excited state [6,7]. The similarities found between the spectroscopic properties of the multimetallic complex and the monometallic specie [11], as well as the comparable emission lifetime with this and other similar monometallic complexes [5,11], and also considering theoretical calculations (vide infra), allow us to attribute the luminescence of $[(CO)_3(phen)Re(\mu\text{-}Br)Re(phen)(CO)_3]^+[(CO)_3Re(\mu\text{-}Br)_3Re(CO)_3]^-$ to the cationic fragment of this complex. However, a minor contribution of the anionic fragment to the spectroscopic properties can be distinguished in both the absorption and emission processes. Supported by the theoretical calculations, the more pronounced absorption shoulder at 300 nm could be attributed to a *d–d* electronic transition on the anionic counterion (see Table 3 and Fig. S2, Supporting information). Regarding the emission process, the major component of the biexponential luminescent decay with longer lifetime is assigned to the MLCT transition of the cationic multimetallic fragment [11,30], while the minor component, with shorter luminescent lifetime, would be related to the emission from the anionic counterion.

3.3. Theoretical calculations

In order to gain a better insight about the nature of the photophysical properties of $[(CO)_3(phen)Re(\mu\text{-}Br)Re(phen)(CO)_3]^+[(CO)_3Re(\mu\text{-}Br)_3Re(CO)_3]^-$, we have performed DFT and TD-DFT calculations. Since the X-rays single crystal structure shows no covalent interaction between the ionic parts of the components, we decided to treat the cation and the anion portions independently. Geometry optimization in both, gas phase and using PCM, resulted in very close agreement with structural data obtained by X-ray diffraction, as shown in Table S1 in the Supporting information. This information suggests that the bridging angle defined by the bromide connecting the two $[(phen)Re(CO)_3]^+$ fragments within the anion is not strongly influenced by the packing within the solid, but instead reflects mainly its electronic structure. In the case of the anion, it is not a surprise that the calculated and experimental distances match closely due to the rigidity conferred by the three bridging bromides.

TD-DFT excitation results for the $[(CO)_3Re(\mu\text{-}Br)_3Re(CO)_3]^-$ anion show that light absorption occurs always under 300 nm, implying that this specie does not contribute to the spectra in the visible region. Fig. 5b shows the transitions within the anion as computed using the PCM model corresponding to dichloromethane. In contrast, TD-DFT results for the $[(CO)_3(phen)Re(\mu\text{-}Br)Re(phen)(CO)_3]^+$ cation show that the absorption for this specie occurs mainly around 400 nm in the gas phase (Fig. 5a), and the energy of this transition is sensitive to the polarity of the media, as expected for MLCT processes. Table 3 shows the main component for each transition for both, cation and anion. These theoretical calculations, in addition to the experimental results, confirm the MLCT nature of the absorption on the cation and the d-d nature of the transition of the anion. Fig. 6 shows the DFT computed frontier orbitals of the $[(CO)_3(phen)Re(\mu\text{-}Br)Re(phen)(CO)_3]^+$ cation. A quantitative picture arises by examining the condensed-to-atom Fukui distributions f_k^- and f_k^+. Table 4 reports main contributions (higher than 3.0%) associated to each atomic center in both distributions for the case of the cationic species. Within a perturbative approach, these results point out the initial local propensity of the system to experience a given charge transfer process. Result indicates that electron releasing will mainly be associated to (and highly concentrated on) both metal rhenium centers and the bridging bromine atom. A lower contribution to electron releasing is associated to one of the CO ligands in each fragment. In contrast, the acceptor region is symmetrically distributed on both *phen* fragments, including the nitrogen centers and six carbon atoms.

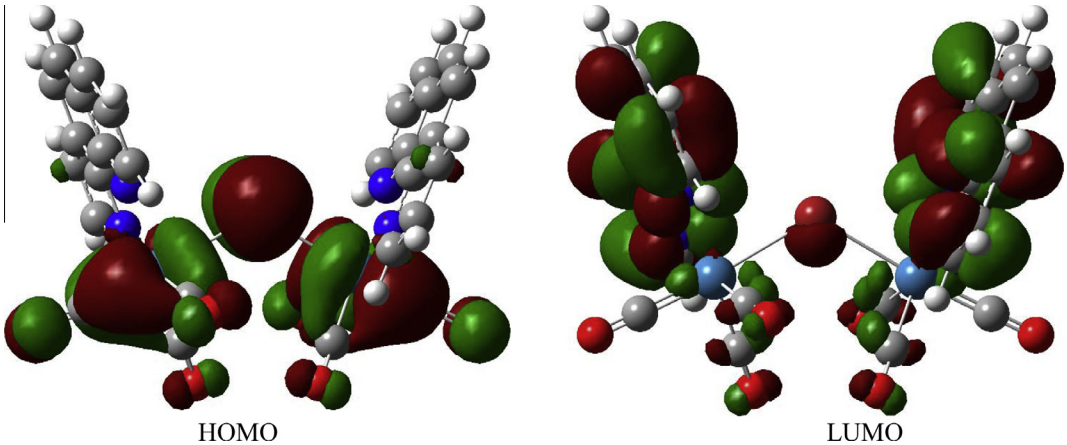

Fig. 6. DFT computed frontier orbitals for the $[(CO)_3(phen)Re(\mu\text{-}Br)Re(phen)(CO)_3]^+$ cation.

Table 4
Main contributions (in percent) from atomic centers to the electron donor and electron acceptor Fukui distributions.

Atom (k)	% contribution to f_k^-	% contribution to f_k^+
Re1	25.5	–
Re2	25.5	–
Br1	20.0	–
C13	3.0	–
O13	4.3	–
C35	3.0	–
O35	4.3	–
N1, N3	–	5.1
N2, N4	–	5.9
C12, C32	–	4.5
C11, C31	–	4.3
C9, C29	–	4.3
C8, C28	–	6.1
C3, C23	–	4.7
C2, C22	–	4.5

Atomic numeration referred to Fig. 1a.

4. Conclusion

Reaction of $(Re(CO)_3(THF)Br)_2$ and 1,10-phenanthroline in toluene in a 1:1 ratio, led to the multimetallic complex $[[(CO)_3(phen)Re(\mu\text{-}Br)Re(phen)(CO)_3][(CO)_3Re(\mu\text{-}Br)_3Re(CO)_3]]\cdot CH_2Cl_2$. The compound possesses two bimetallic complexes as cation and anion, having the Re^I centers bridged through one and three bromides, respectively. Absorption at 375 nm has been assigned to a MLCT band, and excitation at this wavelength produces luminescent emission at 608 nm. The emission lifetimes values, in addition to the capability of generate $O_2(^1\Delta_g)$, suggest the contribution of a triplet state in emission. Finally, by analogy with the spectroscopic properties of closely related model complexes, additionally to theoretical calculations, we can conclude that the luminescence comes mainly from the cationic fragment of the multimetallic complex, $[(CO)_3(phen)Re(\mu\text{-}Br)Re(phen)(CO)_3]^+$.

Acknowledgements

The authors gratefully acknowledge partial financial support of Dirección de Investigación Universidad Andres Bello, grant DI-111-12/R, Comision Nacional de Ciencia y Tecnología, grants FONDECYT 1120865 (AV) and 1140343 (EC) and ACE-03. AV is a member of Financiamiento Basal para Centros Científicos y Tecnológicos de Excelencia FB0807.

Appendix A. Supplementary data

CCDC 1001244 contains the supplementary crystallographic data for $[[(CO)_3(phen)Re(\mu\text{-}Br)Re(phen)(CO)_3][(CO)_3Re(\mu\text{-}Br)_3Re(CO)_3]]\cdot CH_2Cl_2$. These data can be obtained free of charge via http://www.ccdc.cam.ac.uk/conts/retrieving.html, or from the Cambridge Crystallographic Data Centre, 12 Union Road, Cambridge CB2 1EZ, UK; fax: (+44) 1223-336-033; or e-mail: deposit@ccdc.cam.ac.uk. Supplementary data associated with this article can be found, in the online version, at http://dx.doi.org/10.1016/j.poly.2015.05.024.

References

[1] J.V. Caspar, T.J. Meyer, J. Phys. Chem. 87 (1983) 952.
[2] L. Wallace, D.P. Rillema, Inorg. Chem. 32 (1993) 3836.
[3] L. Wallace, D.P. Rillema, Abstr. Pap. Am. Chem. Soc. 205 (1993) 396-INOR.
[4] A.P. Zipp, L. Sacksteder, J. Streich, A. Cook, J.N. Demas, B.A. DeGraff, Inorg. Chem. 32 (1993) 5629.
[5] M. Wrighton, D.L. Morse, J. Am. Chem. Soc. 96 (1974) 998.
[6] A. Cannizzo, A.M. Blanco-Rodríguez, A. El Nahhas, J. Šebera, S. Záliš, J.A. Vlček, M. Chergui, J. Am. Chem. Soc. 130 (2008) 8967.
[7] A. El Nahhas, C. Consani, A.M. Blanco-Rodríguez, K.M. Lancaster, O. Braem, A. Cannizzo, M. Towrie, I.P. Clark, S. Záliš, M. Chergui, A. Vlček, Inorg. Chem. 50 (2011) 2932.
[8] W. Hieber, H. Fuchs, Z. Anorg. Allg. Chem. 248 (1941) 269.
[9] P. Kurz, B. Probst, B. Spingler, R. Alberto, Eur. J. Inorg. Chem. (2006) 2966.
[10] F. Venegas, N. Pizarro, A. Vega, J. Chil. Chem. Soc. 56 (2011) 823.
[11] R.M. Spada, M. Cepeda-Plaza, M.L. Gómez, G. Günther, P. Jaque, N. Pizarro, R.E. Palacios, A. Vega, J. Phys. Chem. C 119 (2015) 10148.
[12] F. Wilkinson, W.P. Helman, A.B. Ross, J. Phys. Chem. Ref. Data 22 (1993) 113.
[13] APEX2, in, Bruker AXS Inc., Madison, Wisconsin, USA, 2001.
[14] G. Sheldrick, Acta Cryst. A 64 (2008) 112.
[15] Frisch, M.J.T., Trucks, G.W.; Schlegel, H. B.; Scuseria, G. E.; Robb, M. A.; Cheeseman, J.R.; Scalmani, G.; Barone, V.; Mennucci, B.; Petersson, G.A.; Nakatsuji, H.; Caricato, M.; Li, X.; Hratchian, H.P.; Izmaylov, A.F.; Bloino, J.; Zheng, G.; Sonnenberg, J.L.; Hada, M.; Ehara, M.; Toyota, K.; Fukuda, R.; Hasegawa, J.; Ishida, M.; Nakajima, T.; Honda, Y.; Kitao, O.; Nakai, H.; Vreven, T.; Montgomery, J.A., Jr.; Peralta, J.E.; Ogliaro, F.; Bearpark, M.; Heyd, J.J.; Brothers, E.; Kudin, K.N.; Staroverov, V.N.; Kobayashi, R.; Normand, J.; Raghavachari, K.; Rendell, A.; Burant, J.C.; Iyengar, S.S.; Tomasi, J.; Cossi, M.; Rega, N.; Millam, N.J.; Klene, M.; Knox, J.E.; Cross, J.B.; Bakken, V.; Adamo, C.; Jaramillo, J.; Gomperts, R.; Stratmann, R.E.; Yazyev, O.; Austin, A.J.; Cammi, R.; Pomelli, C.; Ochterski, J.W.; Martin, R.L.; Morokuma, K.; Zakrzewski, V.G.; Voth, G.A.; Salvador, P.; Dannenberg, J.J.; Dapprich, S.; Daniels, A.D.; Farkas, Ö.; Foresman, J.B.; Ortiz, J.V.; Cioslowski, J.; Fox, D.J., Gaussian 09, in, Gaussian, Inc., Wallingford CT, 2009.
[16] S. Miertuš, E. Scrocco, J. Tomasi, Chem. Phys. 55 (1981) 117.
[17] S. Miertus~, J. Tomasi, Chem. Phys. 65 (1982) 239–245.
[18] W. Humphrey, A. Dalke, K. Schulten, J. Mol. Graphics 14 (1996) 33.
[19] Persistence of Vision Pty. Ltd., Persistence of Vision (TM) Raytracer. Persistence of Vision Pty. Ltd., Williamstown, Victoria, Australia, 2004. http://www.povray.org/.
[20] R.G. Parr, W. Yang, J. Am. Chem. Soc. 106 (1984) 4049.
[21] W. Yang, W.J. Mortier, J. Am. Chem. Soc. 108 (1986) 5708.
[22] R.R. Contreras, P. Fuentealba, M. Galván, P. Pérez, Chem. Phys. Lett. 304 (1999) 405.
[23] P. Fuentealba, P. Pérez, R. Contreras, J. Chem. Phys. 113 (2000) 2544.
[24] E. Chamorro, P. Pérez, J. Chem. Phys. 123 (2005) 114107.
[25] J. Huhmann-Vincent, B.L. Scott, G.J. Kubas, Inorg. Chem. 38 (1998) 115.
[26] A.C. Filippou, B. Lungwitz, G. Kociok-Köhn, I. Hinz, J. Organomet. Chem. 524 (1996) 133.
[27] M.T. Costello, P.W. Schrier, P.E. Fanwick, R.A. Walton, Inorg. Chim. Acta 212 (1993) 157.
[28] R.S. Herrick, C.J. Ziegler, A. Çetin, B.R. Franklin, Eur. J. Inorg. Chem. 2007 (2007) 1632.
[29] R.L. Davis, N.C. Baenziger, Inorg. Nucl. Chem. Lett. 13 (1977) 475.
[30] Z. Si, X. Li, X. Li, H. Zhang, J. Organomet. Chem. 694 (2009) 3742.